PATTERN SYNTHESIS OF CONFORMAL ARRAYS BY A MODIFIED PARTICLE SWARM OPTIMIZATION

W.-T. Li [1, *], Y.-Q. Hei [2], and X.-W. Shi [1]

[1]Science and Technology on Antenna and Microwave Laboratory, Xidian University, Xi'an, Shaanxi 710071, China

[2]State Key Laboratory of Integrated Services Networks, Xidian University, Xi'an, Shaanxi 710071, China

Abstract—A method of designing a cylindrical conformal array with shaped-beam and reconfigurable dual-beam using a modified particle swarm optimization algorithm is proposed in this paper. The proposed algorithm is easy to implement and efficient to be used in synthesizing conformal arrays with digital attenuators and digital phase shifters. Moreover, the proposed synthesis has taken the actual active element patterns into account, which can reduce the error between computation and realization. Good agreement can be obtained between the desired patterns and the synthesized patterns.

1. INTRODUCTION

Conformal antenna arrays are becoming increasingly important in the designs of future radar and communication systems [1–8]. This is because they can provide benefits such as visual unobtrusiveness, non-interference between aerodynamic performance and the performance of antenna. Microstrip patch antennas are often used as the array element because of their thin profile, light weight, and low cost. What's more, they can be easily made to conform to the structure.

Synthesis of conformal arrays continues to be of interest to researchers in the field. Pattern synthesis techniques developed for linear and planar arrays do not work well with conformal arrays. To deal with this problem, a variety of techniques that have been put forward. In [9], a constrained least-squares optimization was employed

to synthesize two-dimensional elliptical and large three-dimensional conformal arrays. In [10], the simulated annealing technique was developed for the synthesis of antenna patterns of circular arc arrays. A generalized projection method has been proposed in [11] for the conformal array synthesis. [12] investigated the Bezier representations for the multiobjective optimization of conformal array amplitude weights. Besides, based on adaptive array method, an efficient algorithm was proposed to synthesize arbitrary array pattern [13]. Since, if the array is conformal to a curved surface, the radiating elements are directed in different directions, posing unique challenges in the synthesis of antenna arrays. Therefore, it is desirable to design a high-performance and efficiency algorithm in the conformal array synthesis problem. Due to the flexibility and efficiency of the evolutionary optimization algorithms such as the genetic algorithm, ant colony optimization, and particle swarm optimization, they are widely employed for the antenna array pattern synthesis in recent years [14–25]. Moreover, in many practical scenarios, it is required that single array antenna can radiate multiple radiation patterns [26–30].

The particle swarm optimization (PSO) algorithm is a kind of evolutionary computational technology inspired by the intelligent behavior of organisms, which is put forward by learning from the behaviors of bird flocking or fish schooling in searching for food. As an alternative tool to the well known genetic algorithm, PSO has the advantages of simpleness, easy realization, and low computation load memory. Thus, PSO has been extensively investigated and applied to the optimization problem of both continuous space and discrete space.

In this paper, an efficient modified particle swarm optimization (MPSO) is employed to the synthesis of conformal arrays. Furthermore, a stacked microctrip antenna is simulated and fabricated. Then, as the array element, it is used to build the cylindrical arrays. During the synthesis process, different from the most optimization in reported literatures, which assume the elements of the array are represented by isotropic point sensors or the element pattern can be modeled as a cosine function, the proposed synthesis has taken the actual active element pattern into account. By considering the effects of mutual coupling, the error between computation and realization can be reduced. A 20-element cylindrical conformal array with a null-shaped beam pattern and a reconfigurable dual-beam pattern are synthesized to show the effectiveness and flexibility of the proposed algorithm. Besides, digital attenuator and digital phase shifter are adopted during the proposed synthesis. This may prompt the feasibility of the proposed method applied in practical scenarios.

2. PROBLEM FORMULATION

Assuming an array of $M \times N$ elements locate over a cylindrical surface of radius R, as shown in Fig. 1, where M and N are the number of elements in the φ-direction and z-direction, respectively. The angular region of the cylindrical array extends from $-\varphi_0$ to φ_0 and the angular spacing between consecutive elements is fixed to be $2R\varphi_0/M - 1$ in the φ-direction.
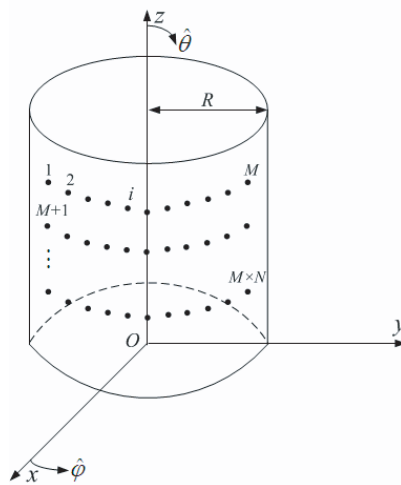

Figure 1. A graphical representation of the antenna element distribution conformal to the cylindrical surface.

The far-field radiation pattern produced by this $M \times N$ elements placed on the cylinder can be expressed as

$$F(\theta, \varphi) = \sum_{n=1}^{N} \sum_{m=1}^{M} I_{mn} f_{mn}(\theta, \varphi)$$
$$\times \exp\left[jk\left[R\sin\theta\cos(\varphi - \varphi_{mn}) + z_{mn}\cos\theta\right] + j\psi_{mn}\right] \quad (1)$$

where I_{mn} is the real value representing the element excitation current amplitude, ψ_{mn} is the excitation current phase, $f_{mn}(\theta, \varphi)$ is the individual element pattern, k is the free-space wave number and φ_{mn}, z_{mn} are the individual coordinates in the φ-direction and z-direction, respectively. It should be noted that in the synthesis examples later, both the excitation current amplitude I_{mn} and the element excitation phase ψ_{mn} are chosen as optimization variables.

In the pattern synthesis process of 20-element cylindrical conformal array with a deep notch on one side, the cost measure to be minimized is defined as the least mean squares of the excess far field magnitude above the specified level, which can be written as

$$fitness1 = \left(\frac{1}{M_s} \sum_{m=1}^{M_s} \left[U\left(e_d\left(\theta, \varphi\right)\right) \times e_d\left(\theta, \varphi\right)^2 \right] \right)^{\frac{1}{2}} \tag{2}$$

$$e_d\left(\theta, \varphi\right) = F_o\left(\theta, \varphi\right) - F_d\left(\theta, \varphi\right) \tag{3}$$

where $F_o\left(\theta, \varphi\right)$ and $F_d\left(\theta, \varphi\right)$ are normalized patterns obtained by optimization and the desired pattern, respectively. M_s is the total sample points, and $U\left(t\right)$ is the unit step function.

3. MODIFIED PARTICLE SWARM OPTIMIZATION

As one powerful and promising optimization method, PSO is capable of solving difficult multidimensional optimization problems in various fields. In this section, standard PSO algorithm is presented first. Then, a modified version of PSO algorithm is proposed with the purpose of promoting the efficiency and performance of PSO.

3.1. Standard PSO Algorithm (SPSO)

In PSO, each particle has a position vector $\mathbf{x_i} = (x_{i1}, x_{i2}, \ldots x_{iD})$ in the D-dimensional search space and moves through the problem space, with the moving velocity of each particle represented by a position vector $\mathbf{v_i} = (v_{i1}, v_{i2}, \ldots v_{iD})$. Each particle keeps track of its own best position $\mathbf{pbest_i} = (pbest_{i1}, pbest_{i2}, \ldots pbest_{iD})$ and the best position among all the particles obtained so far in the population $\mathbf{gbest} = (gbest_1, gbest_2, \ldots gbest_D)$, which are given by:

$$v_{id}^{\tau+1} = wv_{id}^{\tau} + c_1 r_{1d}\left(pbest_{id}^{\tau} - x_{id}^{\tau}\right) + c_2 r_{2d}\left(gbest_d^{\tau} - x_{id}^{\tau}\right) \tag{4}$$

$$x_{id}^{\tau+1} = x_{id}^{\tau} + v_{id}^{\tau+1} \tag{5}$$

where c_1 and c_2 are acceleration constants and r_{1d} and r_{2d} are uniformly distributed random numbers in $[0, 1]$. w is the inertia weight factor and in general, it is set according to the following equation:

$$w = w_{\max} - \frac{w_{\max} - w_{\min}}{T} \cdot \tau \tag{6}$$

where T is the maximum number of iterations, τ is the current iteration number. $w_{\max}$ and $w_{\min}$ are the maximum and the minimum value of the weighting factor respectively.

3.2. Modified PSO Algorithm (MPSO)

Standard PSO converges rapidly during the initial stages of a global search. However, around global optimum, the search will become very slow. The direct reason for this is that the global best particle passively depends on the best solution in each iteration. In fact, in nature or human society, a leader in a swarm has the responsibility and task to search more regions to accumulate knowledge and experience to lead the swarm. Similarly, as the guided particle, the global best particle should search more regions actively to reduce the overhead simulation costs. According to this inspiration, if the global best particle can be replicated into several copies and each of them can search in an independent manner, then the searching efficiency can be greatly increased.

To accomplish this goal, the clonal selection principle provides an efficient approach [31]. Thus, the global best particle will undergo the clonal selection operation. The number of clones and hypermutation operation can be respectively defined as:

$$N_c = round(\beta N_b) \tag{7}$$

$$gbest_d^* = gbest_d^\tau + 0.1\,(x_{d\min} - x_{d\max})\,Gauss(0,1) \tag{8}$$

where β is the multiplying factor, N_b is the total number of particles, and $round\,(\cdot)$ is the operator that rounds its argument toward the closest integer. $x_{d\min}$ and $x_{d\max}$ are the lower and upper limit of the dth dimensional variable. $gbest_d^\tau$ is the global best position at the τth iteration before hypermutation. $Gauss(0,1)$ is a random Gaussian variable with zero mean and unitary standard deviation.

The steps of the MPSO are given as follows:

Step 1: Initialize the population of P individuals and evaluate their fitness.

Step 2: Compare each particle's evaluation value with its own best **pbest$_i$** evolved so far. The best evaluation value among the **pbest$_i$** is denoted as **gbest**.

Step 3: Update velocity and position according to Eqs. (4) and (5).

Step 4: Clone and mutate the global best particle according to Eqs. (7) and (8). Then, update the global best particle.

Step 5: Repeat Steps 2–4 until a stopping criterion, such as a sufficiently good solution being discovered or a maximum number of generations being completed, is satisfied. The best scoring individual in the population is taken as the final answer.

4. NUMERICAL RESULTS

4.1. Array Element Antenna Design

With a center frequency of 3.2 GHz and a bandwidth exceeding 10%
(VSWR $\leq$ 2) when in isolation, a compact stacked antenna is designed.
The geometry of the stacked array element antenna is given in Fig. 2(a),
which is fabricated on two layers with relative permittivity of 2.65. The
radii of the antenna on the bottom layer and top layer are 15.2 mm and
14.9 mm, respectively. The thicknesses of the top and bottom layers are
all 2.5 mm. The antenna is fed by a standard SMA coaxial connector
from the bottom. Fig. 2(b) shows the photograph of the fabricated
antenna.

As shown in Fig. 3, the measured impedance bandwidth (VSWR $\leq$
2) by Agilent N5230A network analyzer is from 3.0 to 3.36 GHz

(a)   (b)

Figure 2. (a) Geometry of the coaxial-fed, stacked patch antenna,
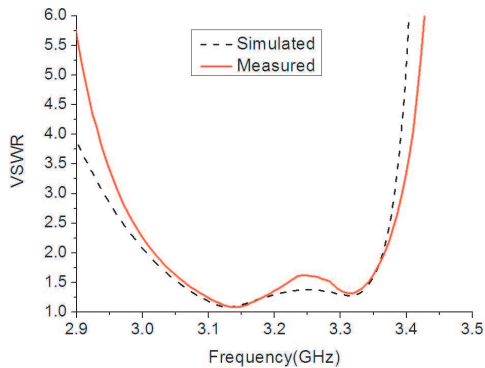and (b) photograph of the fabricated antenna.

Figure 3. Simulated and measured VSWR for the antenna.

(11.32%). There is a good agreement between simulated and measured results. Therefore, the designed antenna can fully satisfy the demanded requirements.

4.2. Synthesis of Pattern Nulling of A Cylindrical Antenna Array

In order to demonstrate the superiority of MPSO in the conformal array pattern synthesis, in each simulation, the performance of MPSO is compared with SPSO and GA. The parameters used in SPSO and GA are selected the same as those used in MPSO, which ensures a fair comparison in computation efficiency and solution quality. What's more, the optimum phase excitation values are quantized between $-180°$ and $180°$ with $5.625°$ per step for 6-bit digital phase shifters. Then, the final phase excitation is:

$$phase_d = round\left(\frac{phase_c}{360/2^5}\right) \cdot \left(360/2^5\right) \qquad (9)$$

where $phase_c$ is the element phase excitation without considering quantization of the digital phase shifter and $round\left(\cdot\right)$ is the same operator as defined in (7). Similarly, the optimum amplitude excitation values are varied in the range 0–1 in steps of $1/2^5$ of a 5-bit digital attenuator.

It is well known that the broad nulls are needed when the direction of arrival of the unwanted interference may vary slightly with time or may not be known exactly, and where a comparatively sharp null would require continuous steering for obtaining a reasonable value for the signal-to-noise ratio. To illustrate the broad-band interference suppression capability of the MPSO, the pattern having a broad null located at $-47°$ with $\Delta\varphi_i = 5°$ is designed.

We consider a 20-element cylindrical array with half-wavelength interelement spacing in φ-direction. The cylinder under consideration has a length of 100 mm and radius of 500 mm. The configuration of cylindrical array is shown in Fig. 4. To take the mutual coupling
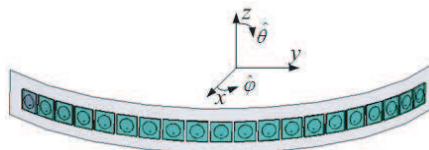

Figure 4. Configuration of the conformal antenna array.

into account, all the active element patterns will be imported into (1). Since the excitation amplitude and the excitation phase of each element are to be optimized, there are totally 40 variables in the optimization process. It is desired that the sidelobe level should be lower than $-20\,\mathrm{dB}$ and the null depth level should be deeper than $-40\,\mathrm{dB}$.

For design specifications, the following parameters have been selected for the proposed algorithm: population size $Q = 40$; generation $T = 3000$; inertia weight factor w is set by (6) with $w_{\max} = 0.9$ and $w_{\min} = 0.4$, acceleration constant $c_1 = 2.0$ and $c_2 = 2.0$. For GA, the crossover probability and mutation probability are selected as 0.8 and 0.02 respectively. Fig. 5 shows normalized absolute pattern
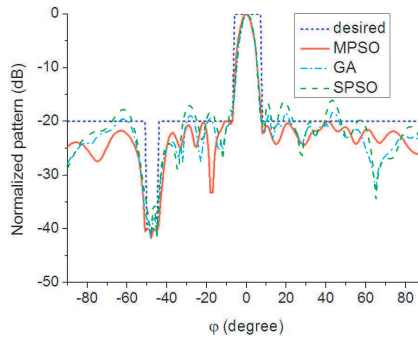

Figure 5. Radiation pattern for the null-shaped beam synthesis.

Table 1. Element excitations obtained by using MPSO for null-shaped beam synthesis.

Element Number	Amplitude Excitation	Phases Excitation	Element Number	Amplitude Excitation	Phases Excitation
1	0.43750	129.375	11	0.84375	16.875
2	0.31250	−78.750	12	0.96875	45.000
3	0.15625	−174.375	13	0.96875	78.750
4	0.21875	16.875	14	0.87500	123.750
5	0.46875	−33.750	15	0.53125	−106.875
6	0.53125	−163.125	16	0.75000	−56.250
7	0.50000	95.625	17	0.56250	61.875
8	0.84375	95.625	18	0.75000	−180.000
9	0.81250	33.750	19	0.43750	−50.625
10	1.00000	50.625	20	0.50000	135.000

of different algorithms. The required amplitude distributions using 5-bit digital attenuator and phase distributions using 6-bit digital phase shifter for the patterns obtained by MPSO are listed in Table 1. The average maximum sidelobe level (MSLL) and cost function evaluations (N_f) of the three algorithms over 20 independent runs are illustrated in Table 2. It is evident that MPSO can accurately produce the nulling pattern with dominated speed while SPSO and GA cannot satisfy the design specification. Fig. 6(a) depicts the comparison between the radiation patterns obtained by MPSO and the full wave simulation results from Ansoft HFSS v11.0. The good agreement between those two results validates our method. In addition, to illustrate the effect of amplitude and phase quantization, a comparison between the patterns with amplitudes and phases before and after the quantization is shown in Fig. 6(b). As can be seen, the maximum sidelobe level is a bit higher after quantization of the excitation amplitudes and phases.

Table 2. Performance comparisons of different algorithms for null-shaped beam synthesis.

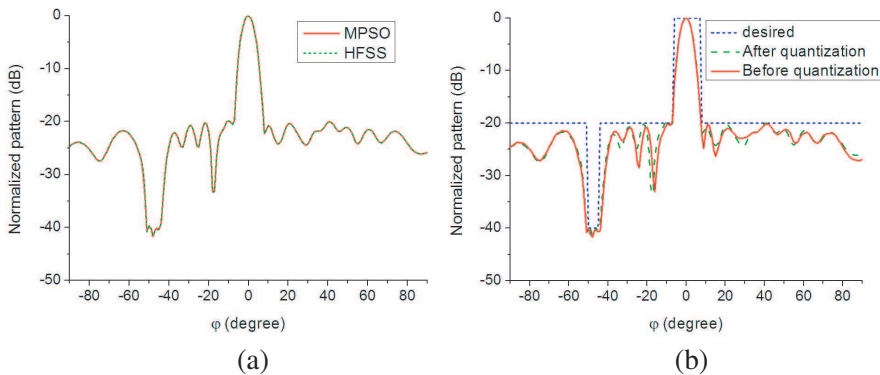| Method	Best fitness value	N_f
GA	2.4944	156480
SPSO	2.5445	155120
MPSO	0.0000	98840

Figure 6. (a) A comparison between the optimized array pattern by MPSO and the exact pattern simulated via HFSS and (b) a comparison between the patterns with amplitudes and phases before and after quantization.

5. EXTENSION TO RECONFIGURABLE ARRAYS

In this part, the proposed method is further extended to the pattern synthesis problems of reconfigurable array to validate its efficiency. For the synthesis of reconfigurable dual-beam pattern, the MPSO is used to generate a pencil beam and a flat-topped beam with a common amplitude distributions and varying phase distributions. Since the optimized targets are different in synthesizing the pencil beam problem and the reconfigurable problem, a different fitness function is constructed as:

$$fitness2 = fitnessp + fitnessf \tag{10}$$

where *fitnessp* is the least mean squares of the excess far field magnitude above the specified level for the pencil beam pattern as defined in (2) and *fitnessf* is the fitness for the flat-topped pattern, which can be defined in the following manner. For each field sample point in shaped-beam regions, the relative error is the difference between the actual pattern obtained by optimization and the desired pattern over M_{sh} total sample points as defined in (11). The least mean square measure is used to represent the overall error pattern as:

$$Esh = \left(\frac{1}{M_{sh}} \sum_{m=1}^{M_{sh}} \left[e_d \left(\theta, \varphi \right)^2 \right] \right)^{\frac{1}{2}} \tag{11}$$

Moreover, the least mean squares of the excess far field magnitude above the specified level in the side-lobe region is:

$$Esl = \left(\frac{1}{M_{sl}} \sum_{m=1}^{M_{sl}} \left[U \left(e_d \left(\theta, \varphi \right) \right) \times e_d \left(\theta, \varphi \right)^2 \right] \right)^{\frac{1}{2}} \tag{12}$$

where M_{sl} is the sample points in the side-lobe region. Then, the fitness function can be defined as:

$$fitnessf = w_s \times Esh + Esl \tag{13}$$

where w_s is a weighting parameter that can be used to emphasize the shaped-beam regions.

In this part, the dual-beam pattern of cylindrical antenna array with the same array configuration of the first example is investigated. For the pencil-shaped beam, the excitation phases are determined by the array theory to focus the beam in the desired scan direction. Nevertheless, the excitation phases varies in the rang $[-180°, 180°]$ to form the flat-topped beam. There are also 40 variables to be optimized including 20 excitation amplitudes and 20 excitation phases. The weighting factor w_s in (13) is chosen as $w_s = 7.8$. The rest parameters

in the optimization process are selected the same as those in the first example.

It is desired that the flat-top main beam of $30°$ and the sidelobe level should be lower than $-15\,\mathrm{dB}$. The sidelobe of the pencil beam should be lower than $-19\,\mathrm{dB}$. The required common amplitude distributions using 5-bit digital attenuator and phase distributions using 6-bit digital phase shifter for the dual-beam patterns obtained by MPSO are listed in Table 3. The normalized dual-beam patterns in the azimuth plane are depicted in Fig. 7. The results obtained by the three results are listed in Table 4. It can be seen that, there is a very good agreement between the desired and obtained results
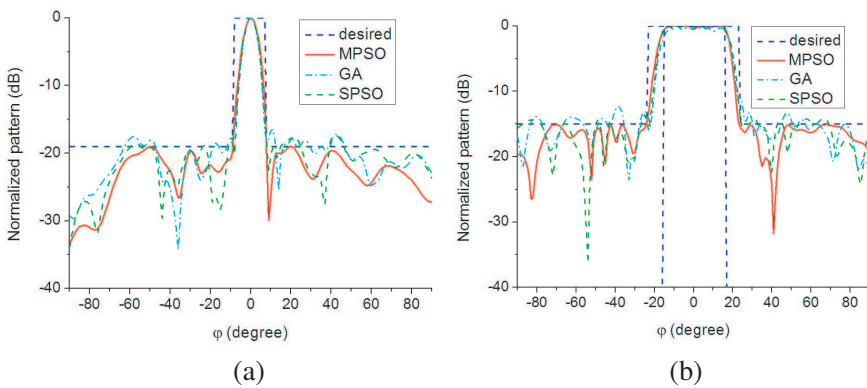

Figure 7. Radiation patterns for the dual-beam array, (a) pencil beam and (b) flat-topped beam.
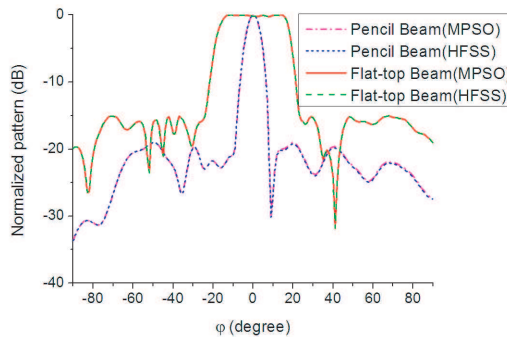

Figure 8. A comparison between the optimized array pattern by MPSO and the exact pattern simulated via HFSS.

Table 3. Element excitations obtained by using MPSO for dual-beam synthesis.

Element Number	Amplitude Excitation	Phases Excitation	Element Number	Amplitude Excitation	Phases Excitation
1	0.15625	163.125	11	0.87500	61.875
2	0.21875	90.000	12	0.90625	33.750
3	0.50000	45.000	13	0.78125	45.000
4	0.40625	−95.625	14	0.71875	45.000
5	0.46875	−146.250	15	0.59375	157.500
6	0.68750	151.875	16	0.50000	−180.000
7	0.81250	78.750	17	0.31250	−140.625
8	0.75000	84.375	18	0.37500	−11.250
9	0.78125	56.250	19	0.09375	−39.375
10	0.81250	118.125	20	0.18750	140.625

Table 4. Final results obtained by GA, SPSO and MPSO.

Method	Pencil Beam	Flat-topped Beam	
	MSLL(dB)	MSLL(dB)	Ripple(dB)
GA	−16.4671	−12.3041	0.2675
SPSO	−17.3631	−13.5783	0.5147
MPSO	−19.0338	−15.0654	0.9978

Table 5. Performance comparisons of different algorithms for dual-beam synthesis.

Method	Best fitness value	N_f
GA	1.4009	143880
SPSO	1.1184	151360
MPSO	0.7212	63120

using MPSO. The comparison of the radiation patterns obtained by MPSO optimization and simulation employing HFSS is shown in Fig. 8. Besides, the average best fitness value and cost function evaluations (N_f) of the four algorithms over 20 independent runs are illustrated in Table 5. It is clear that the proposed algorithm can find optimal solutions within a faster convergent speed.

6. CONCLUSION

In this paper, the optimizations of a null-shaped beam pattern and a reconfigurable dual-beam pattern of a cylindrical array are presented. The proposed synthesis has taken the actual active element patterns in the optimization process to reduce the error between computation and realization. Additionally, to apply amplitude and phase excitations obtained by our method into practice without further quantization, the design method takes the values of digital attenuator and digital phase shifter during synthesis. The procedure and the results of the optimizations show that the proposed algorithm is able to achieve the optimum design for specified design criterions in an effective manner. The accuracy and the robustness of the algorithm validate its potential application in the antenna designs for a wide class of electromagnetic applications.

ACKNOWLEDGMENT

REFERENCES

1. Stotler, M. S. and J. E. Wheeler, "Compact conformal patch antenna," United States Patent, No. US2004/0070536A1, Apr. 15, 2004.

2. Vaskelainen, L. I., "Constrained least-squares optimization in conformal array antenna synthesis," *IEEE Trans. Antennas Propagt.*, Vol. 55, 859–867, 2007.

3. He, Q. Q., H. D. He, and H. Lan, "An efficient pattern synthesis method for cylindrical phased array antennas," *Journal of Electromagnetic Waves and Applications*, Vol. 23, No. 4, 473–482, 2009.

4. Zhang, Y. J., S. X. Gong, and Y. X. Xu, "Radiation pattern synthesis for arrays of conformal antennas mounted on an irregular curved surface using modified genetic algorithms," *Journal of Electromagnetic Waves and Applications*, Vol. 23, No. 10, 1255–1264, 2009.

5. Wincza, K., S. Gruszczynski, and K. Sachse, "Conformal four-beam antenna arrays with reduced sidelobes," *Electron. Lett.*, Vol. 44, 174–175, 2008.

6. Dohmen, C., J. W. Odendaal, and J. Joubert, "Synthesis of conformal arrays with optimized polarization," *IEEE Trans. Antennas Propagt.*, Vol. 55, 2922–2925, 2007.

7. Park, P. K. and R. S. Robertson, "Electronically scanned dielectric covered continuous slot antenna conformal to the cone for dual mode seeker," United States Patent, No. US6653984B2, Nov. 25, 2003.

8. He, Q. Q., B. Z. Wang, and W. Shao, "Radiation pattern calculation for arbitrary conformal arrays that include mutual-coupling effects," *IEEE Trans. Propagt. Mag.*, Vol. 52, 57–63, 2010.

9. Ferreira, J. A. and F. Ares, "Pattern synthesis of conformal arrays by the simulated annealing technique," *Electron. Lett.*, Vol. 33, 1187–1189, 1997.

10. Bucci, O. M., G. D'Elia, and G. Romito, "Power synthesis of conformal arrays by a generalized projection method," *IEE Proc. Microw. Antennas Propagt.*, Vol. 142, 467–471, 1995.

11. Boeringer, D. W. and D. H. Werner, "Bezier representations for the multiobjective optimization of conformal array amplitude weights," *IEEE Trans. Antennas Propagt.*, Vol. 54, 1964–1970, 2006.

12. Zhou, P. Y. and M. A. Ingram, "Pattern synthesis for arbitrary arrays using an adaptive array method," *IEEE Trans. Antennas Propagt.*, Vol. 47, 862–869, 1999.

13. Xu, Z., H. Li, and Q. Z. Liu, "Pattern synthesis of conformal antenna array by the hybrid genetic algorithm," *Progress In Electromagnetics Research*, Vol. 79, 75–90, 2008.

14. Zhou, H. J., B. H. Sun, J. F. Li, and Q. Z. Liu, "Efficient optimization and realization of a shaped-beam planar array for very large array application," *Progress In Electromagnetics Research*, Vol. 89, 1–10, 2009.

15. Li, R., L. Xu, X. W. Shi, N. Zhang, and Z. Q. Lv, "Improved differential evolution strategy for antenna array pattern synthesis problems," *Progress In Electromagnetics Research*, Vol. 113, 429–441, 2011.

16. Rocca, P., L. Poli, G. Oliveri, and A. Massa, "Synthesis of time-modulated planar arrays with controlled harmonic radiations," *Journal of Electromagnetic Waves and Applications*, Vol. 24, No. 5–6, 827–838, 2010.

17. Zhang, S., S. X. Gong, and P. F. Zhang, "A modified PSO for low sidelobe concentric ring arrays synthesis with multiple

constraints," *Journal of Electromagnetic Waves and Applications*, Vol. 23, No. 11–12, 1535–1544, 2009.

18. Eirey-Perez, R., M. Alvarez-Folqueiras, J. A. Rodriquez-Gonzalez, F. J. Ares-Pena, "Arbitrary footprints from arrays with concentric ring geometry and low dynamic range ratio," *Journal of Electromagnetic Waves and Applications*, Vol. 24, No. 13, 1795–1806, 2010.

19. Fernandez-Delgado, M., J. A. Rodriquez-Gonzalez, R. Iglsias, S. Barro, and F. J. Ares-Pena, "Fast array thinning using global optimization method," *Journal of Electromagnetic Waves and Applications*, Vol. 24, No. 16, 2259–2271, 2010.

20. Li, F., Y. C. Jiao, L. S. Ren, Y. Y. Chen, and L. Zhang, "Pattern synthesis of concentric ring array antennas by differential evolution algorithm," *Journal of Electromagnetic Waves and Applications*, Vol. 25, No. 2–3, 421–430, 2011.

21. Villegas, F. J., "Parallel genetic-algorithm optimization of shaped beam converge areas using planar 2-D phased arrays," *IEEE Trans. Antennas Propagt.*, Vol. 55, 1745–1753, 2007.

22. Dib, N., S. K. Goudos, and H. Muhsen, "Application of Taguchi's optimization method and self-adaptive differential evolution to the synthesis of linear arrays," *Progress In Electromagnetics Research*, Vol. 102, 159–180, 2010.

23. Lanza, M., J. R. Perez, and J. Basterrechea, "Synthesis of planar arrays using *s* modified particle swarm optimization algorithm by introducing a selection operator and elitism," *Progress In Electromagnetics Research*, Vol. 93, 145–160, 2009.

24. Ou Yang, J., Q. R. Yuan, F. Yang, H. J. Zhou, Z. P. Nie, and Z. Q. Zhao, "Synthesis of conformal phased array with improved NSGA-II algorithm," *IEEE Trans. Antennas Propagt.*, Vol. 57, 4006–4009, 2009.

25. Ebehart, R. and J. Kennedy, "A new optimizer using particle swarm theory," *Proceedings of the Sixth International Symposium on Micro Machine and Human Science*, 39–43, 1995.

26. Mahanti, G. K., A. Chakraborty, and S. Das, "Design of fully digital controlled reconfigurable array antennas with fixed dynamic range ratio," *Journal of Electromagnetics Waves and Applications*, Vol. 21, No. 1, 97–106, 2006.

27. Mak, A. C. K., C. R. Rowell, and R. D. Murch, "Low cost reconfigurable Landstorfer planar antenna array," *IEEE Trans. Antennas Propagt.*, Vol. 57, 3051–3061, 2009.

28. Jamlos, M. F., O. A. Aziz, T. A. Rahman, M. R. Kamarudin,

P. Saad, M. T. Ali, and M. N. M. Tan, "A reconfigurable radial line slot array (RLSA) antenna for beam shape and broadside application," *Journal of Electromagnetic Waves and Applications*, Vol. 24, No. 8–9, 1171–1182, 2010.

29. Ali, M. T., M. N. Md Tan, T. B. A. Rahman, M. R. B. Kamarudin, M. F. Jamlos, and R. Sauleau, "A novel of reconfigurable planar antenna array (RPAA) with beam steering control," *Progress In Electromagnetics Research B*, Vol. 20, 125–146, 2010.

30. Mahanti, G. K., S. Das, and A. Chakraborty, "Design of phase-differentiated reconfigurable array antennas with minimum dynamic range ratio," *IEEE Antennas Wirel. Propag. Lett.*, Vol. 20, 2620–264, 2006.

31. De Castro, L. N. and F. J. VonZuben, "Learning and optimization using the clonal selection principle," *IEEE Tran. Evolutionary Computation*, Vol. 6, 239–251, 2002.